

In situ microscopy and MIR-spectroscopy as non-invasive optical sensors for cell cultivation process monitoring

Background: The use of modern sensors for online monitoring has become increasingly important in biotechnology. For bioprocess analysis the chemical and physical environment as well as the biological component itself must be monitored in detail and in real-time. **Results:** Modern non-invasive optical sensors allow reliable predictions of the current process status just in time. Two sensors, one for the biological and one for monitoring the chemical system of a CHO cell cultivation process, are presented. With an *in situ* microscope, cell count and morphology are monitored, to assess the efficiency of the cell growth up to a cell concentration of $1.4 \cdot 10^7$ cells/ml. An infrared sensor was used to analyze glucose concentration profiles. Both sensors can be used as *in situ* non-invasive sensors. **Conclusion:** With both sensors, reliable online monitoring of CHO cell cultivation process is feasible that react immediately to changes in process conditions. Higher product quality and more efficient processes can be realized.

In cell cultivation processes it is important to have consistent product quality and detailed process documentation. Therefore the monitoring of many process variables is necessary. The most important indicators are the concentration of glucose and lactate, partial pressure of oxygen (pO_2), temperature and pH value for the chemical environment and cell concentration, viability, morphology for the biological environment.

In the last two decades various sensors have been developed and established. Process analytics for cell cultivation processes is divided into two general modes of operation: in the first, samples are withdrawn from the process via a sterile sampling device and analyzed offline. Analytical techniques for the analysis of offline samples exist in a huge variety. One disadvantage of this approach is the contamination risk during the sample taking procedure. Another disadvantage is the delay between the time of sampling and the time when the analysis data is available. This results in great difficulties when establishing a process control system. The second mode of operation is online monitoring via

in situ sensors, directly interfaced to the process. The advantage of online measurement is the continuous monitoring or the monitoring at high sampling rates. Additionally the sensor response is rapid or even instantaneous. However, only a few online sensors besides pO_2 and pH are available for bioprocess monitoring.

Online sensors that are physically separated from the process, for example by a glass window, are of special interest. Non-invasive sensors are advantageous over invasive by having no direct interaction with cell cultivation broth. Examples for non-invasive measurement techniques include near infrared (NIR) and mid infrared (MIR) spectroscopy as well as 2D fluorescence spectroscopy and *in situ* microscopy [1–3].

Another important issue is, that a precise characterization of a bioprocess requires a precise characterization of the chemical environment of the process, for example, concentration of analytes in the media, as well as the biological component (e.g., the cells) [4–6]. A way of measuring the concentrations of chemical components in the cultivation

Christian Lüder¹,
Patrick Lindner¹,
David Bulnes-Abundis¹,
Shaobin M Lu¹, Tim Lücking¹,
Dörte Solle^{*1}
& Thomas Scheper¹

¹Leibniz Universität Hannover, Institut für Technische Chemie, Callinstr. 5, 30167 Hannover, Germany

*Author for correspondence:
solle@iftc.uni-hannover.de



Key Terms

Mid infrared: Online prediction of glucose concentration based on multivariate data analysis.

Imageprocessing: Determination of cell count and morphological information on online microscopic images.

broth with optical, non-invasive sensors is the spectroscopy in the NIR and MIR wavelength range [7]. Examples that are already documented in the literature include the determination of glucose and lactate concentration [8] and many other components. For characterization of biological components optical sensors can be used as well: an indirect characterization is possible with 2D fluorescence spectroscopy [9], while a direct observation of the biological components can be achieved using an *in situ* microscope (ISM). With *in situ* microscopy, images of the cell suspension can be acquired at arbitrary sampling rates and in different magnifications. Using automated **image processing** algorithms, changes in cell concentration or cell morphology [10] can be monitored in real time over the whole cell cultivation process. A method for determination of cell concentration is already presented for a flow-through microscopic multitesting system [11] with *Saccharomyces cerevisiae*.

In this study a sensor system consisting of MIR spectroscopy and *in situ* microscopy is presented. With this sensor system cell concentration and morphology as well as glucose concentration are measured in real time and non-invasively during the entire cell cultivation process.

A CHO cell line is used for cultivation, as a benchmark process for biopharmaceutical industry [12–14]. This model organism is a convenient example to establish new sensor systems for large-scale bioprocess analytics.

Materials & methods

Cultivation

A non-producing cell line, CHO-K1 (CHO cell line, Cell Culture Technology, University of Bielefeld, Germany) was cultivated in a commercially available serum-free

medium CHOMACS CD (Miltenyi Biotec, Bergisch Gladbach, Germany) for 164 h. CHOMACS CD is the same medium as TC-42 (TeutoCell AG, Bielefeld, Germany). The culture medium contains 7.59 g/l glucose and is free of hypoxanthine, thymidine and glutamine. CHOMACS CD was supplemented with glutamine to a total concentration of 8 mM to promote cell growth. Glutamine was supplemented shortly before inoculation because of its decomposition [15]. The cultivation setup was carried out according to Sandor *et al.* [16].

Cultivations were carried out in a 10-l bioreactor (Biostat® Cplus, Sartorius Stedim Biotech GmbH, Göttingen, Germany) with a working volume of 7.5 l. After inoculation the bioreactor had a cell concentration of $4 \cdot 10^5$ cells/ml at the beginning. Temperature was maintained at 37°C and pH was monitored by an electrochemical electrode (Easy Ferm Plus K8, Hamilton Messtechnik GmbH, Höchst, Germany) and maintained at 7.1 by addition of Na_2CO_3 and by CO_2 aeration.

The bioreactor was pressurized (0.1 bar) to increase the oxygen uptake. Dissolved oxygen was monitored via an amperometric electrode (Oxyferm FDA, Hamilton Messtechnik GmbH, Höchst, Germany) and maintained at 40% by automatic aeration via ring sparger with an air or air–oxygen mixture. To keep foam formation and mechanical stress for the cells at a minimum, the maximum aeration rate was limited to 0.5 l/min. The stirring rate was fixed at 200 rpm.

Samples were taken by a steam sterilized sample port at 4 h intervals during the whole cultivation. During the night time the samples were collected at every 8 h. All reference assays were conducted in triplicate. The analyzed variables including their observed ranges are listed in Table 1. Total cell concentration and the amount of viable and dead cells were determined directly after sampling with a Cedex cell counter (innovates AG, Bielefeld, Germany). All samples were centrifuged (5 min, 1000 g, 4°C) to remove cells from the medium for further analysis. Glucose, lactate, glutamine and glutamate were measured with an YSI 2700 biochemistry analyser (YSI Inc., Yellow Spring, OH, USA).

Table 1. Offline analysis and observed ranges.

Analyte	Range	Unit
Glucose	0–9	g/l
Lactate	0–4	g/l
Glutamine	0–1100	mg/l
Glutamate	0–325	mg/l
Total cell concentration	$0-1.8 \times 10^7$	N/ml
Viable cell concentration	$0-1.6 \times 10^7$	N/ml
Viability	10–100	10^{-5} cells/ml

Glucose and lactate concentrations were determined immediately after the centrifugation step. Glutamine and glutamate samples were stored at -20°C and measured at the end of each cultivation.

In situ microscopy

For the non-invasive monitoring of cell concentrations an *in situ* microscope [1] was used. Many ISM versions were constructed, tested and applied in the past which differed mainly in the measuring zone setup and the illumination unit [11,17,18]. With ISM many different applications were already established [19–22]. The following experiment was carried out with the most recent development called ISM-TT. The main differences in contrast to prior ISM devices are the optical elements which were changed from finite to infinite optics. Further on, in the ISM-TT linear stages M-111.1DG (Physik Instrumente GmbH & Co. KG, Karlsruhe, Germany) were used, that allow for a precise focussing and a precise settings of the measuring zone height. The microscope system was based on the principle of a transmitted light/bright-field microscope (TB-ISM) with infinite optics. A green LED ($I = 20\text{ mA}$, $\lambda \approx 516\text{ nm}$, $I_v = 24.000\text{ mcd}$, Winger Electronics GmbH & Co, Dessau, Germany) was used for illumination. The pictures were acquired by a pco.pixelfly (PCO AG, Kelheim, Germany) CCD camera through a tenfold magnifying objective. The ISM was connected to 25-mm standard Ingold® port. The measurement concept of the ISM is shown in the article by Akin *et al.* [23].

During the cultivation one acquisition cycle occurs every hour. An acquisition cycle consists of two steps: an image acquisition procedure lasting for 7 min and a waiting period until the next acquisition cycle (53 min). When the acquisition procedure starts the measuring zone was set to a height of $30\ \mu\text{m}$. Such a small gap was necessary to achieve monolayers of cells within the measurement zone. During the image acquisition procedure 200 focused images (Figure 1E) and afterwards 200 defocused images (Figure 1A & C) are acquired. The time between every image is 1 s and the exposure time setting of the camera was $95\ \mu\text{s}$. After every acquisition procedure the height of the measuring zone was opened to $1000\ \mu\text{m}$ during the waiting period. The consequence of this was an increased flow through the measurement zone which in turn minimizes the attachment of cells to the optical parts inside the zone.

Two different image processing algorithms were used to analyze the acquired images. The first one operates on the defocused images, which were used for the determination of cell concentration and the second algorithm performs an analysis of the cell morphology using the focused images.

The algorithm for the defocused images is simple: it performs a binarization using a fixed threshold to separate the overexposed cell centers from the background. On the resulting binary image white dots represent the cell centers while all areas that do not contain cells are black. The cells per image can easily be counted on that binary image by using a standard border tracking algorithm that yields the count of objects (Figure 1B & D). This simple algorithm and the defocused acquisition technique were chosen because of high cell concentrations appearing during the cell cultivation process. At high cell densities the cells tend to contact each other directly or even overlap. Those cell clusters pose a potential problem for any image processing algorithm. On defocused images the cell center is much brighter than the rest of the cell and by using the above mentioned algorithm even cell clusters were detected as single objects without the need for a complicated separation method (Figure 1C & D). This approach leads to robust and reliable results for the cell count even if the entire image was covered with cells. On the other hand if an in focus acquisition technique was used this would lead to great problems with the cluster separation that are hard to overcome. The cell count per acquisition cycle was calculated by averaging the cell count of all 200 defocused images to consider the variance of cell numbers inside the measuring zone during an acquisition cycle.

While the above mentioned algorithm yields a precise cell count, no information about the cell size and shape can be gained from the defocused images. For this reason a second algorithm was designed that operates on the focused images. Key step of this algorithm is an edge detection, in contrast to the algorithm for defocused images. First the images were preprocessed using a contrast stretch followed by a median filter (kernel size 3) to minimize image noise. After the preprocessing steps a SUSAN [24] edge detection was performed. The edge detection includes a binarization step. By using a border tracking algorithm the objects were detected on the binary image. Here the size and shape information of the objects was preserved in contrast to the objects detected on the defocused images. For each object the size, roundness (cell morphology) and diameter was calculated. The objects found include single cells as well as clusters. To obtain size and shape information on the single cells only the clusters were excluded from further analysis by a roundness criterion.

The size distribution gives an idea about the age of the cells, because older cells tend to be bigger. The morphology, especially the roundness, is also an indication for cell age.

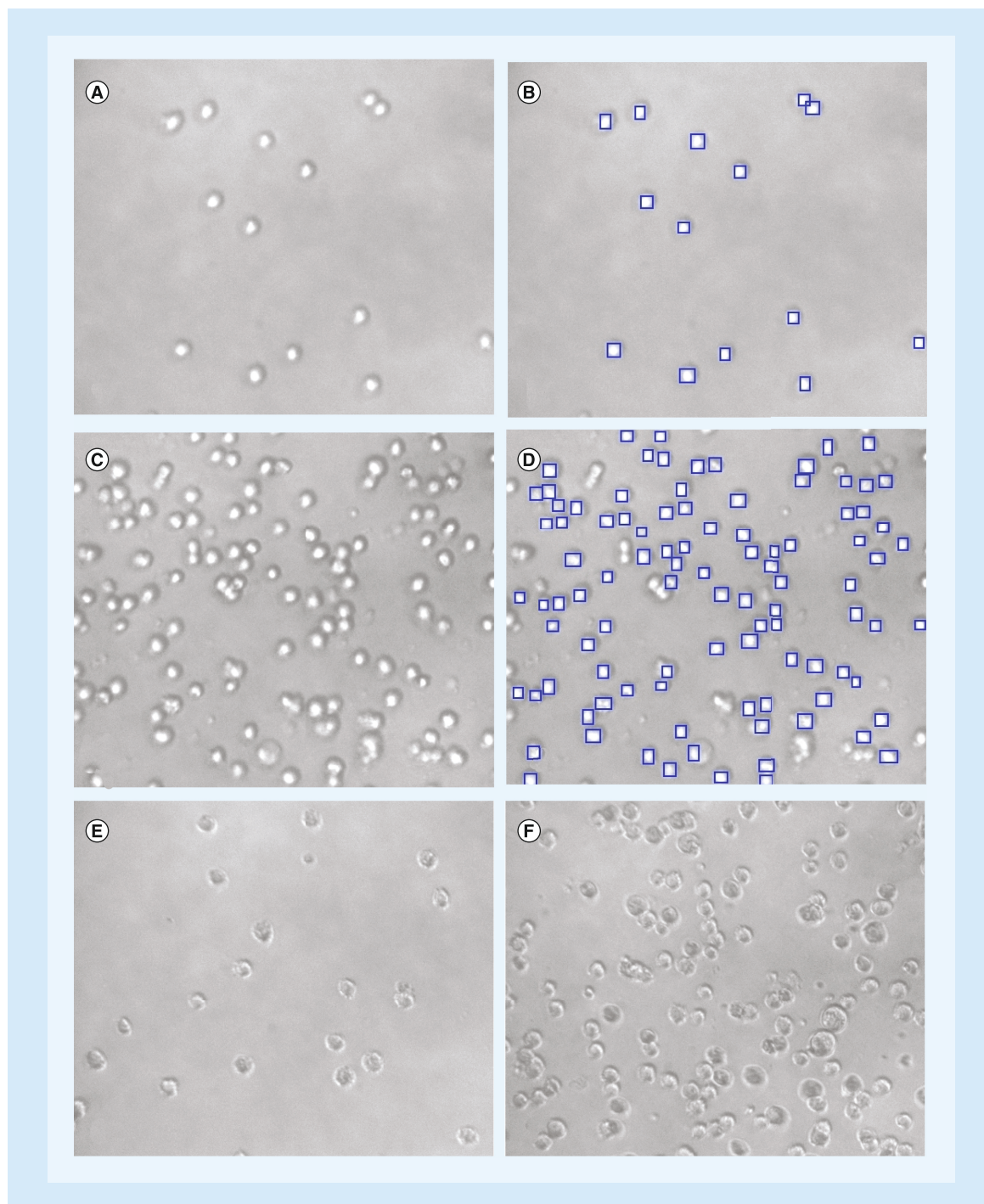


Figure 1. *In situ* microscope images. (A, B, E) After 79 h; **(C, D, F)** after 162 h. **(A–D)** Defocused images, **(B)** and **(D)** are the same pictures as **(A)** and **(C)** after cell determination; **(E)** and **(F)** are focused images.

MIR spectroscopy

MIR spectra were collected using a MATRIX-MF (Bruker Optik GmbH, Ettlingen, Germany) with a mercury cadmium telluride detector cooled by a peltier element. A diamond ATR probe (length 120 mm, diameter 13.5 mm, adapter for 25 mm) with two reflections (art photonics GmbH, Berlin, Germany)

was introduced into the reactor through a 25 mm Ingold port and connected via silver halogenide fibre to the spectrometer. The software OPUS 6.5 (Bruker Optik GmbH, Ettlingen, Germany) and SIPAT (Siemens AG) was used for operating the MIR spectrometer. Background spectra of the culture medium at 37°C without any additives were used to calculate the

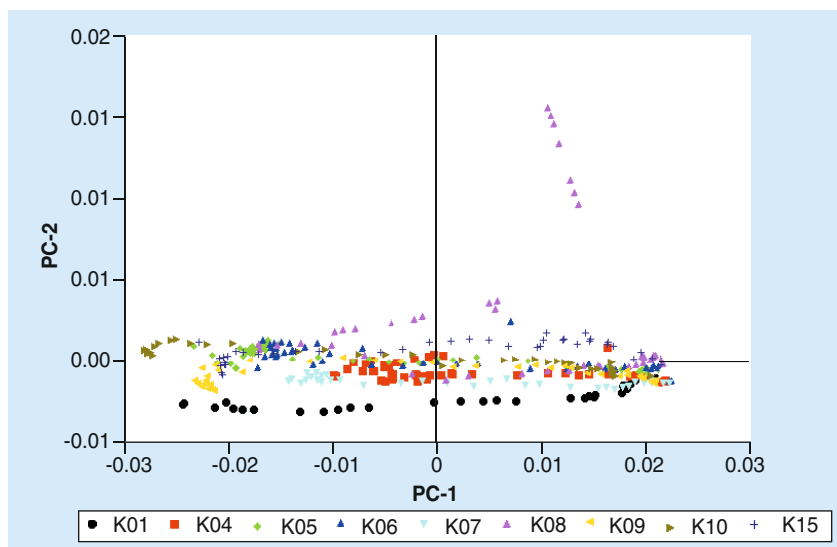


Figure 2. Glucose partial least square score plot of 361 mid infrared spectra from nine different batch and fed-batch cultivations.

absorbance spectra of the single-beam spectra collected continuously every 2 min during cultivation. Each MIR spectrum was compressed of an average of 1000 co-added scans taken at a resolution of 4 cm^{-1} and a speed of 80 kHz in the range of $3000\text{--}700\text{ cm}^{-1}$. Absorbance spectra corresponding to the time of offline measurements are used for calibration.

Spectral data were analysed with the Unscrambler X (Camo, Oslo, Norway). Principal component analysis was carried out on baseline corrected and centered absorbance MIR spectra in the range of $1200\text{--}950\text{ cm}^{-1}$, to identify spectral outliers, important trends within a batch as well as batch to batch variations. Baseline corrected data give the best results compared with other pre-processing methods, such as standard normal variate, detrending or deviation. A calibration model was built for glucose with partial least square regression using the NIPALS algorithm. It was not possible to build a sophisticated model for lactate, glutamine or glutamate.

Nine former cultivation runs with a total of 361 samples were used for calibration. The former cultivation processes were performed as batch or fed-batch cultivations, but in TC-42 medium instead of CHOMACS. In the score plot (Figure 2) all batch and fed-batch cultivations are distributed similarly along the first principal component, only seven samples of cultivation K08 representing a high glucose feed up to 9 g/l were separated by the second principal component. Therefore the inter process variance was very small compared with the intra process variance of the MIR data. The model for glucose was precise, with an RMSEC of 0.23 g/l and an R^2 of 0.99 using four principal components. Four PCs minimize the validation

error to predict unknown process runs. The RMSEV for full cross validation was 0.24 g/l and the test set validation error for predicting an unknown process run was 0.33 g/l. The regression coefficients of the calibration model strongly correlate with the pure component glucose spectra measured in aqueous solution (Figure 3).

Results

This study presents the online measurement of cell density, cell morphology and a prediction of the glucose concentration for a CHO cell cultivation process. During this process, 65,600 images were acquired with the ISM, representing 164 h of the batch cultivation. With the two-step data collection of focused and defocused images, much better results for cell count at higher cell densities and also information about cell morphology were accessible. During the cell cultivation process, 3140 MIR spectra were also recorded and a glucose prediction was generated using a multivariate model.

In Figure 1E a focused image for a low cell concentration of approximately 4.0×10^6 cells/ml is shown next to an image of a high cell concentration of 1.3×10^7 cells/ml in Figure 1F. Changes in the morphology can be observed. In a later stage of the cultivation the cells tend to agglomerate. Furthermore the cell size distribution gets broader and the amount of cell fragments increases. In Figure 4, cell size distributions at two different cultivation time points were shown. At an early time point (97 h) the size distribution is smaller and most of the cells have a diameter of approximately 15 μm . At a later process state (162 h) the size distribution was much broader. More small cells or cell fragments

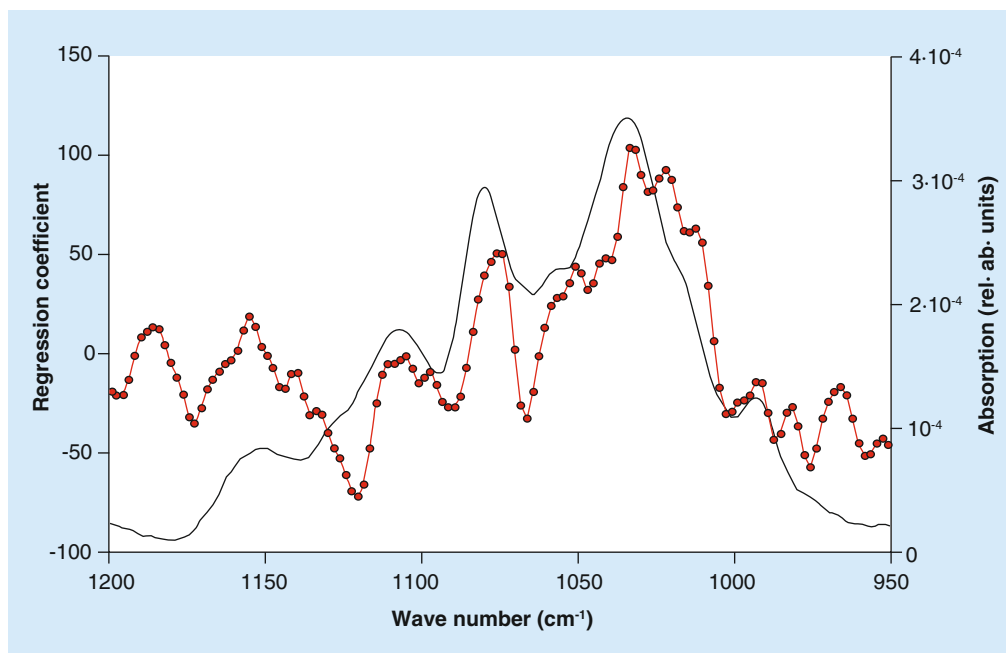


Figure 3. Regression coefficients of glucose partial least square with four PCs (dotted red line) in comparison with pure component glucose spectra (black line).

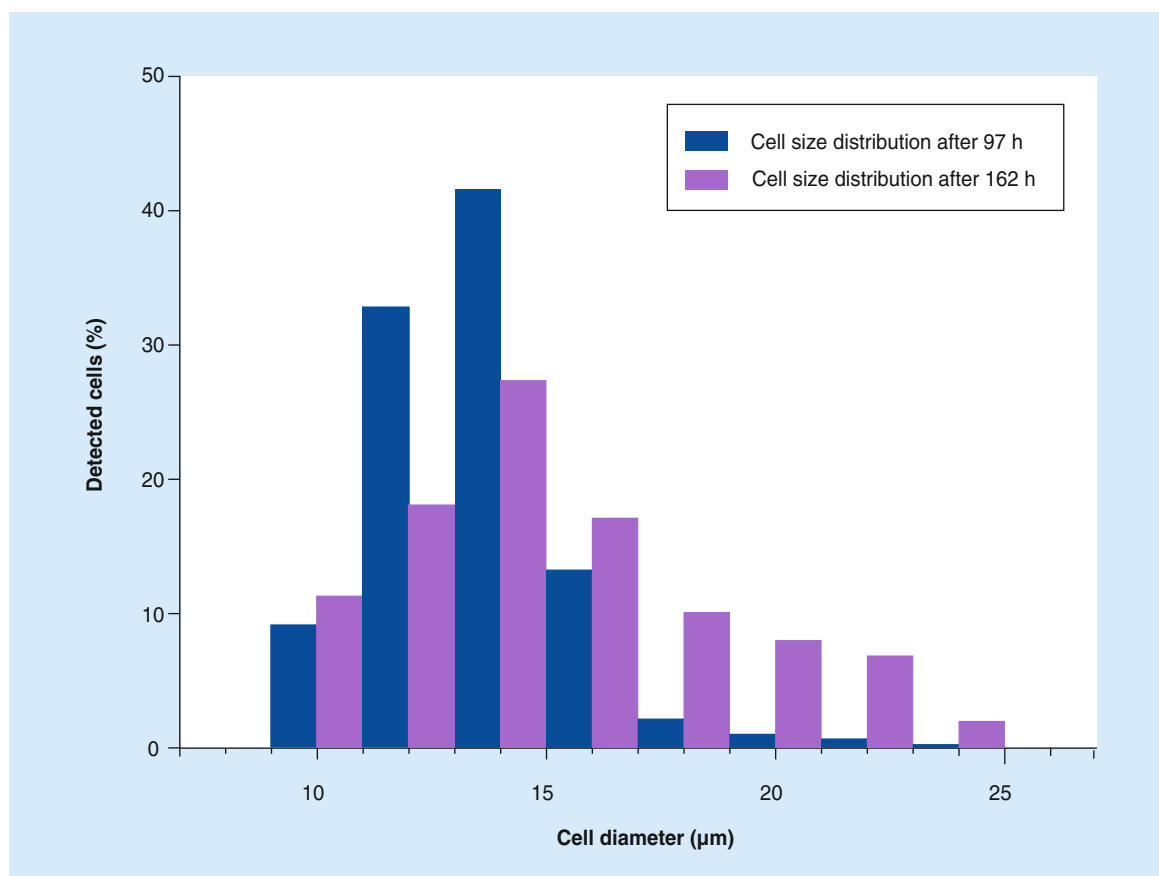


Figure 4. Cell size distribution out of the analyzed defocused images at the beginning and the end of the cultivation.

appear but the largest gain was for cells featuring a diameter over $15\ \mu\text{m}$. This acknowledges the observation that the cells become much larger at later stages of the cultivation process. Cells with a diameter of $24\ \mu\text{m}$ may also be small cell aggregates.

To determine the cell concentration, defocused images were analyzed. The comparison of ISM cell count with offline cell concentration measured with the Cedex cell counter demonstrates that the correlation is not linear. An assumption for this would be the fluid dynamic around the measurement zone. The volumetric flow tends to go around the measurement zone, so that the effective amount of cells inside the zone is lower than in the rest of the reactor. A special amount of cells per measuring cycle is representative for a special cell concentration in this bioreactor and the amount of cells is independent of cell cycle, initial concentration and glucose level. For low cell densities the cells had the tendency not to pass through the measurement zone. While at high cell densities a representative amount of cells were pushed into the measurement zone and the ISM cell count correlates to the offline measurement.

To account for the above mentioned effects a non-linear regression was used as can be seen in Figure 5.

The resulting data points could be fitted by a logarithmic function (Equation 1). The parameters A and B are not in context of cell proliferation, they are considering the fluid dynamic throw the measurement zone. A and B were estimated using the least square sum method: $A = 3.0 \times 10^6 \pm 8.5 \times 10^4$ cells/ml and $B = -6.4 \times 10^6 \pm 3.8 \times 10^5$ cells/ml. The coefficient of determination is $R^2 = 0.98$ and indicates that this model function describes the data very precise. With this calibration the ISM results can be transformed to cell count in cells/ml and be directly compared with reference values. The offline and online cell concentration is shown in Figure 6. The exponential growth is clearly visible followed by a stationary phase beginning at 130 hours which was induced by the lack of glutamine (not shown in Figure 6).

$$\text{CellCount} = A \cdot \ln(\text{CellCount}_{\text{ISM}}) + B \quad (\text{Equation 1})$$

The calculated values of the online measurement were similar to the offline values determined by the Cedex. With the ISM, an online measurement of cell count can be achieved, enabling the monitoring of mammalian cell growth during a batch cultivation process in real time and without sample taking. The presented analysis should be possible in general for spherical cells. For every

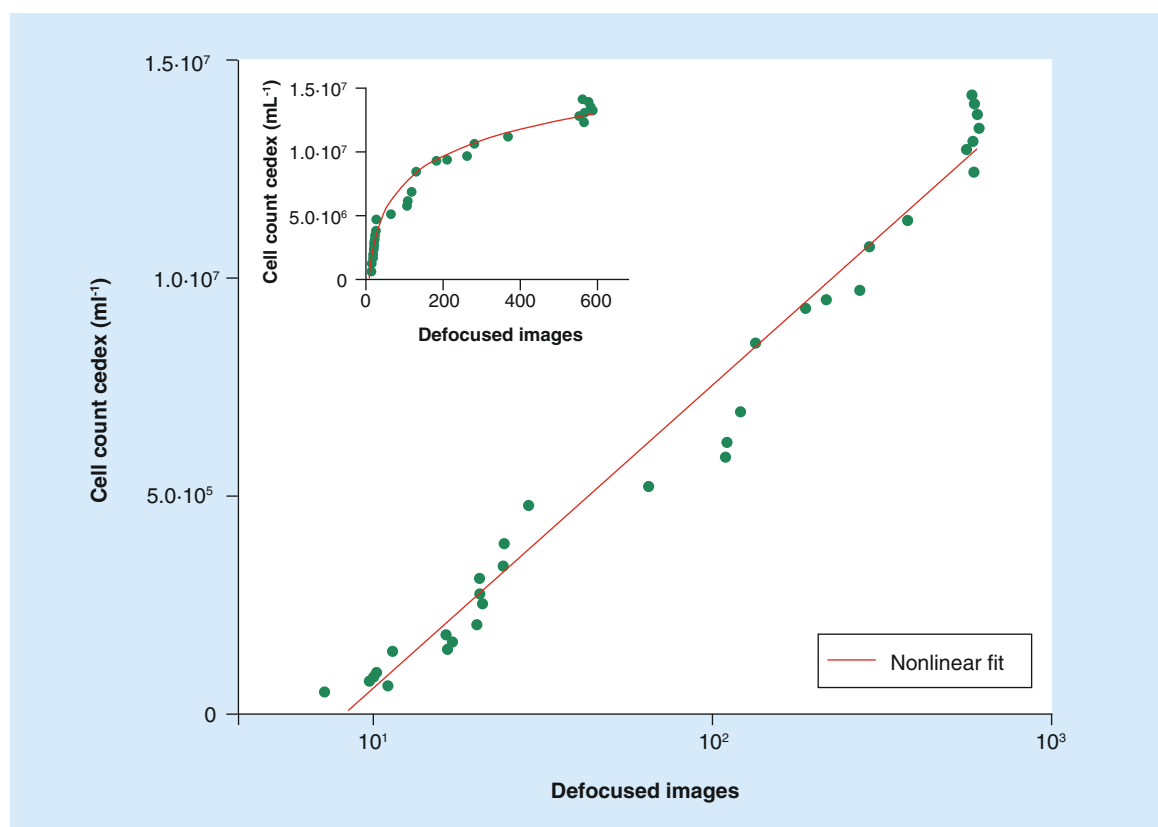


Figure 5. Cedex values plotted against *in situ* microscope data of defocused images, the inset graph with linear scaled axes and the red curve shows a non-linear fit based on a logarithmic equation, the large graph shows the same data with a logarithmic scaled x-axis.

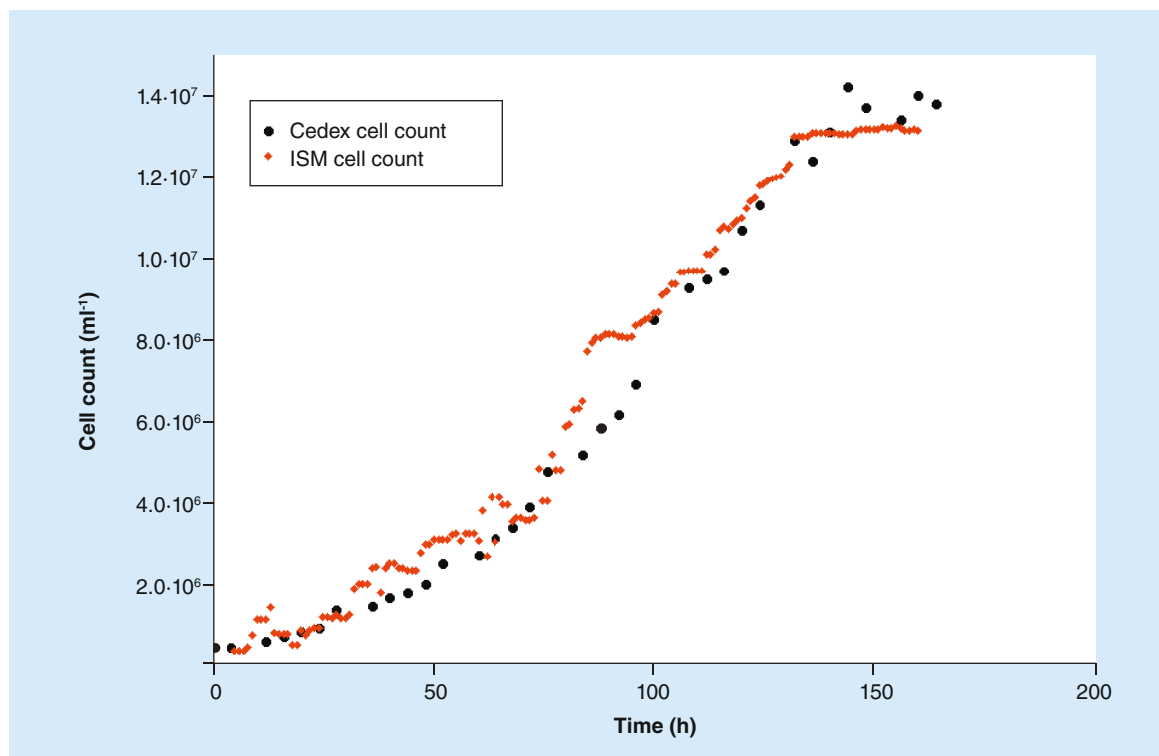


Figure 6. Calculated cell count by *in situ* microscope of defocused images and Cedex cell count as reference.

new cell type a new correlation between ISM values and offline measurements is needed. For a flow-through microscopic multitest system the determination of cell concentration of *S. cerevisiae* with defocused images is already presented [11].

To achieve a non-invasive measurement of glucose concentration in real time, MIR spectroscopy combined with multivariate data analysis was used. Based on historical data of nine cultivation runs, a chemometric calibration was modeled to predict

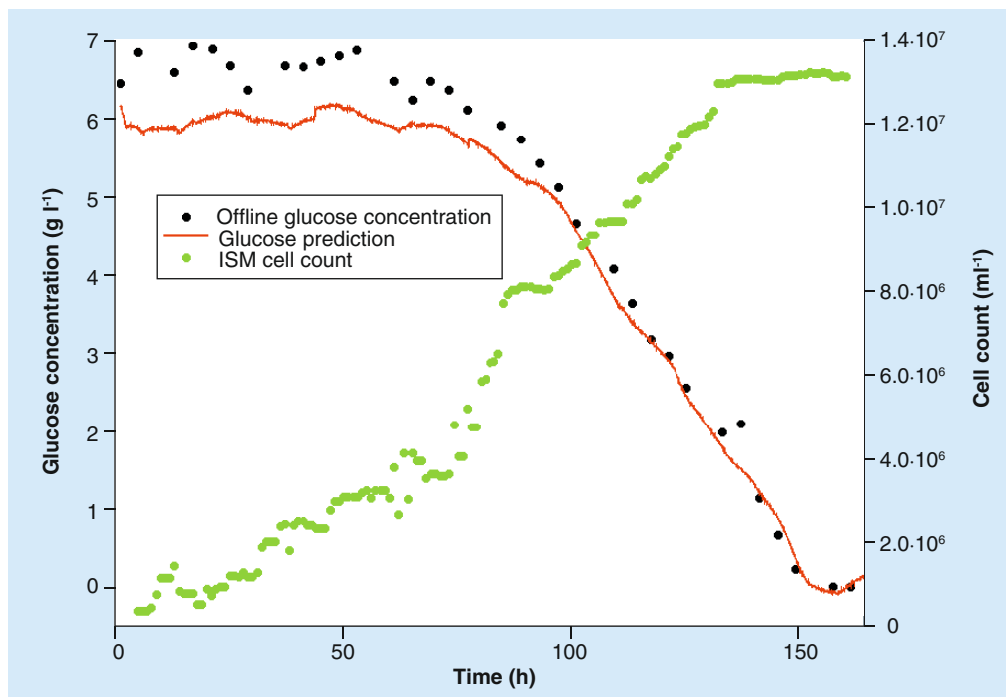


Figure 7. Offline glucose concentration and online glucose prediction together with *in situ* microscope cell count.

glucose concentration of the tenth cultivation process online, based on MIR spectra in Figure 7. In the first 50 h of cultivation the glucose prediction was constant at approximately 6 g/l while during the exponential growth phase in the next 100 h the glucose concentration decreases to 0 g/l successively. The comparison of 39 glucose offline measurements with online predictions results in a prediction error of 0.47 g/l.

In Figure 7 online predictions based on MIR spectra are shown next to offline measurements by YSI and cell count based on ISM measurement and image analysis. It can be seen, that for high glucose concentrations the prediction error and the offline measurement noise is much higher than for small glucose concentrations. The deviation of glucose prediction in the beginning of the process was caused by medium change from TC-42 in calibration processes to CHOMACS in prediction process. However for process control, low glucose concentrations are especially interesting, where online prediction gives very good results.

Glucose consumption can be predicted in real time and therefore a glucose feeding control is possible. For an optimal process control – leading to higher cell density – substrate feeding is essential. Based on online prediction of glucose via MIR-spectroscopy and a reliable multivariate model, a control loop for feeding can be established.

With both techniques together, two important process variables are accessible online. Based on the measurement of cell count by ISM combined with digital image processing algorithms and the prediction of glucose concentration by MIR spectroscopy together with multivariate data analysis, a reliable estimation of the actual process state is feasible – not only to monitor the

process but also to establish a process control, substrate feed and optimal harvest.

Future perspective

In order to make the process analytical technology initiative of the US FDA a success, more reliable online sensors are needed, especially non-invasive ones. The aim is to achieve large-scale fed-batch cultivations even in the field of high cell density cultivations. For this kind of processes simple, reliable and robust analytical methods are required. Using the current sensor system of MIR glucose prediction and ISM determination of cell count and morphology, a self-adjusting process by closed loop control is feasible. Further steps include the calculation of the optimal glucose feed. The optimal feed time can be estimated using the results of the MIR spectra while the optimal amount can be chosen by exact determination of biomass using the ISM. Further efforts in ISM will lead to online measurement of the concentration of dead cells from their morphological properties. With this information the cell viability will also be available. Over the next few years, the aim is to develop online systems for cell cultivation monitoring that do not rely on sample collection and to establish a process control in accordance with process analytical technology.

Financial & competing interests disclosure

The authors have no relevant affiliations or financial involvement with any organization or entity with a financial interest in or financial conflict with the subject matter or materials discussed in the manuscript. This includes employment, consultancies, honoraria, stock ownership or options, expert testimony, grants or patents received or pending, or royalties.

No writing assistance was utilized in the production of this manuscript.

Executive summary

Background

- The development of new online and non-invasive sensor applications for monitoring cell cultivation processes has become increasingly important.

Materials & methods

- A sensor system consisting of mid infrared spectroscopy and *in situ* microscopy was developed and tested during a CHO cell cultivation process. This sensor system allows the measurement of glucose concentration, cell count and cell morphology in real time.

Results & discussion

- With the sensor system presented in this study, a reliable online monitoring of CHO cell cultivation processes is feasible that reacts immediately to changes in process conditions. Higher product quality and more efficient processes can be realized.

References

Papers of special note have been highlighted as:

•• of considerable interest

- 1 Prediger A, Lindner P, Bluma A, Reardon K, Scheper T. *In situ* microscopy. In: *Optical Techniques in Regenerative*

Medicine (Volume 1). Morgan S (Ed.). Taylor & Francis, Boca Raton, USA, 116–141 (2013).

- 2 Rudolph G, Lindner P, Bluma A *et al.* Optical inline measurement procedures for counting and sizing cells in bioprocess technology. In: *Optical Sensor Systems in*

- Biotechnology* (Volume 116). Rao G (Ed.). Springer, NY, USA, 73–97 (2009).
- 3 Höpfner T, Bluma A, Rudolph G, Lindner P, Scheper T. A review of non-invasive optical-based image analysis systems for continuous bioprocess monitoring. *Bioprocess Biosyst. Eng.* 33(2), 247–256 (2010).
 - 4 Bluma A, Höpfner T, Prediger A, Glindkamp A, Beutel S, Scheper T. Process analytical sensors and image-based techniques for single-use bioreactors. *Eng. Life Sci.* 11(4), 1–4 (2011).
 - 5 Belini V, Wiedemann P, Suhr H. *In situ* microscopy: a perspective for industrial bioethanol production monitoring. *J. Microbiol. Methods* 93(3), 224–232 (2013).
 - 6 Beutel S, Henkel S. *In situ* sensor techniques in modern bioprocess monitoring. *Appl. Microbiol. Biotechnol.* 91(6), 1493–1505 (2011).
 - 7 Landgrebe D, Haake C, Höpfner T et al. On-line infrared spectroscopy for bioprocess monitoring. *Appl. Microbiol. Biotechnol.* 88(1), 11–22 (2010).
 - 8 Navratil M, Norberg A, Lembrén L et al. On-line multi-analyzer monitoring of biomass, glucose and acetate for growth rate control of a *Vibrio cholera* fed-batch cultivation. *J. Biotechnol.* 115(1), 67–79 (2005).
 - 9 Ödman P, Johansen C, Olsson L, Gernaey K, Lantz A. Sensor combination and chemometric variable selection for online monitoring of *Streptomyces coelicolor* fed-batch cultivations. *Appl. Microbiol. Biotechnol.* 86(6), 1745–1795 (2010).
- Gives a good overview of *in situ* microscopy.
- 10 Bluma A, Höpfner T, Lindner P et al. *In situ* imaging sensors for bioprocess monitoring: state of the art. *Anal. Bioanal. Chem.* 398(6), 2429–2438 (2010).
 - 11 Rehbock C, Riechers D, Höpfner T et al. Development of a flow-through microscopic multitesting system for parallel monitoring of cell samples in biotechnological cultivation processes. *J. Biotechnol.* 150(1), 87–93 (2010).
 - 12 Kim J, Kim Y, Lee G. CHO cells in biotechnology for production of recombinant proteins: current state and further potential. *Appl. Microbiol. Biotechnol.* 93(3), 917–930 (2012).
 - 13 Walsh G. Biopharmaceutical benchmarks 2010. *Nat. Biotechnol.* 28(9), 917–924 (2010).
 - 14 Hacker D, Jesus M, Wurm F. 25 years of recombinant proteins from reactor-grown cells – where do we go from here?. *Biotechnology advances.* 27(6), 1023–1027 (2009).
 - 15 Tritsch GL, Moore GE. Spontaneous decomposition of glutamine in cell culture media. *Exp. Cell Res.* 28(2), 360–364 (1962).
- A comparable example for mid infrared spectroscopy and online prediction.
- 16 Sandor M, Rüdinger F, Bienert R, Grimm C, Solle D, Scheper T. Comparative study of non-invasive monitoring via infrared spectroscopy for mammalian cell cultivations. *J. Biotechnol.* 168(4), (2013).
 - 17 Prediger A, Bluma A, Höpfner T et al. *In situ* mikroskopie zur online-überwachung von enzymträgern und zweiphasenprozessen. *Chem. Ing. Tech.* 83(6), 884–887 (2011).
 - 18 Havlik I, Lindner P, Scheper T, Reardon K. On-line monitoring of large cultivations of microalgae and cyanobacteria. *Trends Biotechnol.* 31(7), 406–414 (2013).
 - 19 Opitz B, Prediger A, Lüder C et al. *In situ* microscopy for inline monitoring of the enzymatic hydrolysis of cellulose. *Anal. Chem.* 85(17), 8121–8126 (2013).
 - 20 Bluma A, Höpfner T, Rudolph G et al. Adaptation of *in situ* microscopy for crystallization processes. *J. Cryst. Growth.* 311(17), 4193–4198 (2009).
 - 21 Joeris K, Frerichs J, Konstantinov K, Scheper T. *In situ* microscopy: online process monitoring of mammalian cell cultures. *Cytotechnology* 38(1), 129–134 (2002).
 - 22 Anton F, Burzlaff A, Kasper C, Brücknerhoff T, Scheper T. Preliminary study towards the use of *in situ* microscopy for the online analysis of microcarrier cultivations. *Eng. Life Sci.* 7(1), 91–96 (2007).
 - 23 Akin M, Prediger A, Yksel M et al. A new set up for multi-analyte sensing: at-line bio-process monitoring. *Biosens. Bioelectron.* 26(11), 4532–4537 (2011).
 - 24 Smith S, Brady J. SUSAN – a new approach to low level image processing. *Internal Technical Report TR95SMSI* 23(1), 45–78 (1995).